Pulse Oximeter for Low SpO_2 Level Detection Using Discrete Time Signal Processing Algorithm

Sumit Pandey
Center for Reliability Sciences & Technologies, Chang Gung University
Department of Electronic Engineering, Chang Gung University
No. 259, Wen-Hua 1st Road, Guishan District, Taoyuan City, Taiwan, ROC 33302
sumit.pandey.tech@outlook.com

Cher Ming Tan[1]
Center for Reliability Sciences & Technologies, Chang Gung University
Department of Electronic Engineering, Chang Gung University
Institute of Radiation Research, College of Medicine, Chang Gung University
Department of Mechanical Engineering, Ming Chi University of Technology
Department of Urology, Chang Gung Memorial Hospital
No. 259, Wen-Hua 1st Road, Guishan District, Taoyuan City, Taiwan, ROC 33302, No. 5, Fuxing Street, Guishan Dist., Taoyuan City, Taiwan, ROC 33305.
cmtan@cgu.edu.tw

Hsiao-Wen Chen[2]
Department of Urology, Chang Gung Memorial Hospital
Medical College, Chang Gung University

No. 5, Fuxing Street, Guishan Dist., Taoyuan City, Taiwan, ROC 33305. mhc1211@cgmh.org.tw

Yao En Xie
Center for Reliability Sciences & Technologies, Chang Gung University
Department of Electronic, Chang Gung University

[1] **Cher Ming Tan**
Center for Reliability Sciences & Technologies, Chang Gung University
Department of Electronic Engineering, Chang Gung University
Institute of Radiation Research, College of Medicine, Chang Gung University
Department of Mechanical Engineering, Ming Chi University of Technology
Department of Urology, Chang Gung Memorial Hospital
No. 259, Wen-Hua 1st Road, Guishan District, Taoyuan City, Taiwan, ROC 33302, No. 5, Fuxing Street, Guishan Dist., Taoyuan City, Taiwan, ROC 33305.
cmtan@cgu.edu.tw

[2] **Hsiao-Wen Chen**
Department of Urology, Chang Gung Memorial Hospital
Medical College, Chang Gung University
No. 5, Fuxing Street, Guishan Dist., Taoyuan City, Taiwan, ROC 33305.
mhc1211@cgmh.org.tw

No. 259, Wen-Hua 1st Road, Guishan District, Taoyuan City, Taiwan, ROC 33302. h4564000@gmail.com

Jung Hua Tung
Center for Reliability Sciences & Technologies Chang Gung University
Graduate Institute of Mechanical and Electrical Engineering, National Taipei University of Technology
No. 259, Wen-Hua 1st Road, Guishan District, Taoyuan City, Taiwan, ROC 33302, No. 1, Section 3
fred.tung@mail.cgu.edu.tw

Yu-Chuan Kau
Department of Anesthesiology, Chang Gung Memorial Hospital
No. 5, Fuxing Street, Guishan Dist., Taoyuan City, Taiwan, ROC 33305.
yichuan@cgmh.org.tw

Chia-Chih Liao
Department of Anesthesiology, Chang Gung Memorial Hospital No. 5, Fuxing Street, Guishan Dist., Taoyuan City, Taiwan, ROC 33305.
m7141@cgmh.org.tw

ABSTRACT

Oximeter is an important clinical device used for measuring peripheral capillary oxygen saturation (SpO_2) in blood and hence accurate results are needed in order to help physicians predict clinical problems in the initial stage(s) of liver or kidney diagnosis. Different issues associate with the accuracy of SpO_2 and heart rate measurement accuracy are studied in this work. With the understanding of these issues, a new SpO_2 monitoring system is proposed that comprises of a better detection method, novel discrete time signal processing algorithm and a custom-made oximeter probe head. The proposed SpO_2 measurement system is capable of determining low levels of SpO_2 present in human blood and produce the results in a short time that enable real time monitoring of a patient SpO_2. It can also distinguish low level of SpO_2 against background noise.

INTRODUCTION

Oxygen is an important element for human body functions such as metabolisms, respirations and immunity etc. Many clinical diseases are caused by the lack of sufficient oxygen supply, which will affect the normal metabolism of cells [1]. Operation rooms (OR) and intensive care units (ICU) require a continuous oxygen concentration monitoring system, and real-time monitoring of oxygen concentration in blood is an important health check item.

Since 1986, pulse oximeters have been the standard of care for monitoring the oxygen concentration of blood to ensure health and safety of patients [2]. Through the use of a pulse oximeter during an operation, the anesthesiologist ensures that oxygen is sufficiently delivered to the tissue during mechanical ventilation [3]. After the successful deployment of the pulse oximeter in the Operating Room (OR) and Intensive Care Unit (ICU), it is currently being widely used in other hospital units and patient clinics as well. Medical professionals believe that arterial SpO_2 measured by pulse oximetry, will be the fifth vital sign for human [4], as we previously reported the clinical potential for monitoring hemodynamic changes of the acute scrotum [5].

Here SpO_2 is the ratio of oxyhemoglobin in the red blood cells to total hemoglobin, representing the body's ability to carry oxygen. Currently, there are two methods for measuring SpO_2. The first method is to draw blood from arteries and then use a blood gas analyzer [6] to perform electrochemical analysis [7] for the determination of the partial Pressure of Oxygen (PO_2) which is then converted to the peripheral capillary oxygen saturation (SpO_2).

Although blood gas analyzer can determine the exact value of oxygen level in the blood, it uses invasive needles to draw the blood from arteries, and thus it cannot perform continuous monitoring of blood oxygen level. Also, it is time-consuming. Furthermore, the cost is high and requires a trained medical professional to perform the test, and hence it can only be performed in the hospitals.

In the second method, sensor is placed on the point/area of intent and two light signals with different wavelengths are produced using a pair of Light Emitting Diodes (LEDs). These signals pass through the blood vessels of human tissue simultaneously, and the detectors receive the reflected signals from the blood. The ratio of the intensities of the two reflected signals with different wavelengths are then calculated and converted to SpO_2 via a lookup table [8] based on the Beer-Lambert law [9].

While there are many such commercial oximeters available, their limitations can be summarized in Table 1 with their respective reported solutions. All these limitations produce errors in determining the accurate level of SpO_2 which can be overcome by the reported solutions. However, among them, there are two limitations which remain unnoticed, namely the light scattering property of LED and measurement of low SpO_2 level.

TABLE I Limitations and their reported solutions for the commercial oximeter

S/No	Limitation and Causes	Solution
1.	**Motion Artifacts:** Due to the muscles' movement during measurement [10].	Retrospective motion correction technique is employed at the post-process phase using algorithms to eliminate this limitation [11].
2.	**Ambient Light:** Interference of the ambience light by the photodiodes during measurement [12].	A logarithmic amplifier is added in the signal-processing circuitry to subtract the signal components of ambient light or background light from the received signals [13].
3.	**Skin Pigmentation:** Presence of dark skin pigmentation [14].	It can be solved by 'Munsell color tile system'. In addition, human observation is also required [14].
4.	**Abnormal Hemoglobin Molecules:** Detection of the compounds like abnormal hemoglobin or methemoglobin [15].	It can be eliminated by using a ratio of the first derivative of the first two absorbances of hemoglobin and oxyhemoglobin [15].
5.	**Light scattering property of LED:** LED light scattered due to its characteristic of low power and large divergence angle.	Not reported yet.
6.	**Inability to measure the low SpO_2 level:** signal from low SpO_2 become very weak and the background noise can be stronger than the signal.	Not reported yet.

Available oximeters in the market commonly use LEDs for detection of SpO_2, Due to light scattering effects in LED, signal loss or decrease in the signal to noise ratio (SNR) occurs that causes inaccuracy in the measured SpO_2. Detection of low SpO_2 (< 94%) depends on the low-intensity reflected pulse signals, thus its error can be high, and its measurement time is also very long in order to gather sufficient signal information using pulse oximeter. On the other hand, detection of low SpO_2 level is crucial since it indicates abnormal situation in our body.

In this work, a new methodology is developed to address the two aforementioned un-resolved limitations of oximeters. The proposed methodology is described in the following section.

OXIMETER DESIGN METHODOLOGY

The design and development of oximeter in this work can be divided into two paths, namely hardware and software design.

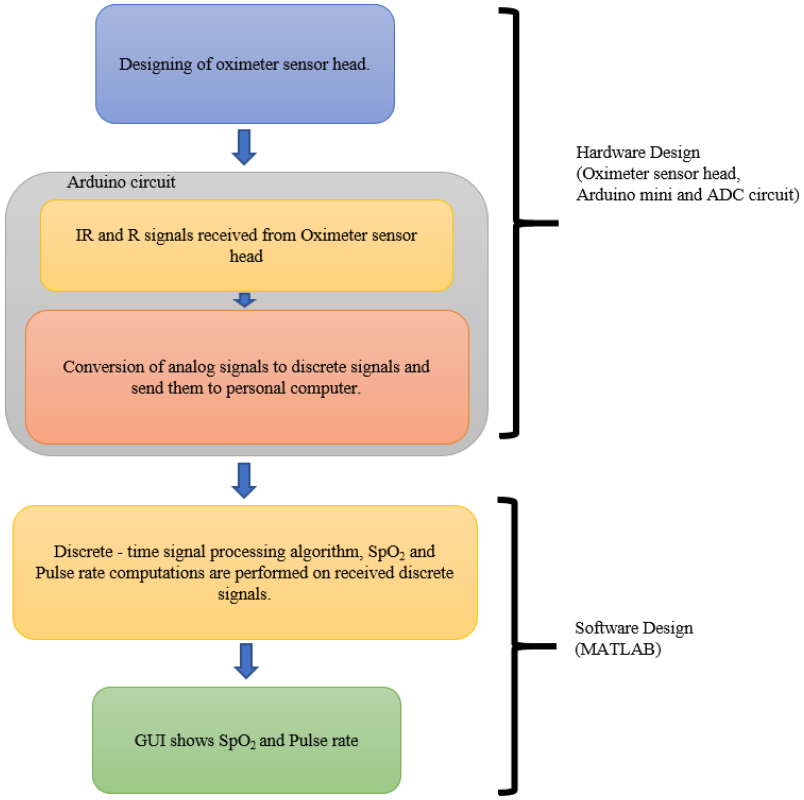

Fig. 1. Research methodology flow chart.

Hardware design includes the designing of oximeter sensor head for transmission of signals. The reflected signals are captured using detectors and the corresponding analog signals are converted to discrete signals for further computation using Arduino pro mini driver circuit. These discrete signals are first filtered using our developed algorithm on MATLAB platform, followed by the computations of SpO_2 and pulse rate. Graphical User Interface (G.U.I.) is designed in the software design path to show the measured SpO_2 level and heart rate. Fig. 1 shows the flow of the oximeter system that is developed in this work.

A. Hardware Design

The hardware module can be divided into sensor and circuit modules as shown in Fig. 2.

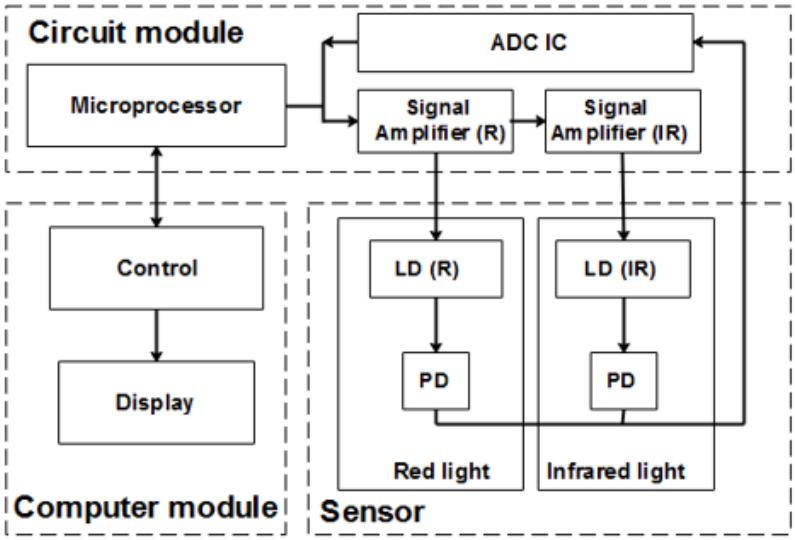

Fig.2 Hardware architecture of oximeter.

The sensor module is a custom-made oximeter sensor probe head fabricated using 3D printing as shown in Fig. 3(a), and it consists of Red (R) and Infrared (IR) light laser diodes (LD) and two photodiodes (PD) placed at a distance from the LD as computed from the optical reflection path. Laser diodes are used so as to eliminate the issue of light scattering in LEDs. For safety consideration, the laser diodes (LD) are low power and it is pulsing so that maximum laser light intensity incident on human tissues are keep within the acceptable limit (20mW to 40 mW) with limited maximum pulsed current for the LDs [16].

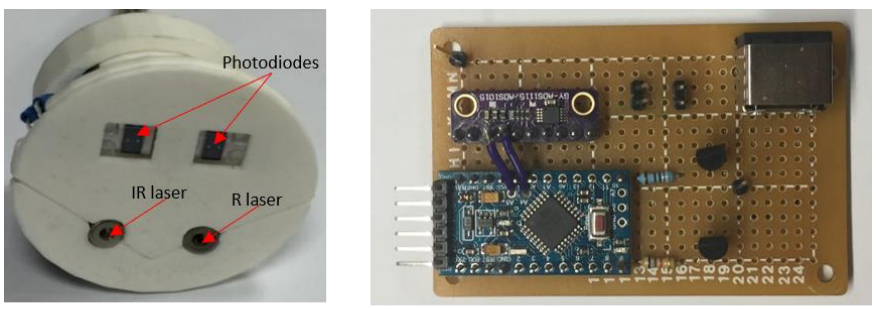

(a) (b)

Fig. 3 (a). Oximeter sensor's probe head, (b). Arduino driven circuit for SpO2 measurement

Fig. 3(b) shows the circuit module that consists a microprocessor (Arduino pro mini), analog to digital converter IC (ADS1115/ ADS105) and transistors. Arduino pro mini microprocessor is used for controlling the emissions of IR and R laser diodes, and the photodiodes are to receive the reflected IR and R signals. Conversion of the received analog signals into the discrete signals is done using analog to digital converter (ADC) IC. These converted signals are then sent to the Microprocessor for discrete time signal processing (DTSP).

B. Software Design

Fig. 4 shows the signal processing algorithm for DTSP, and it consists of three principal steps as explained below.

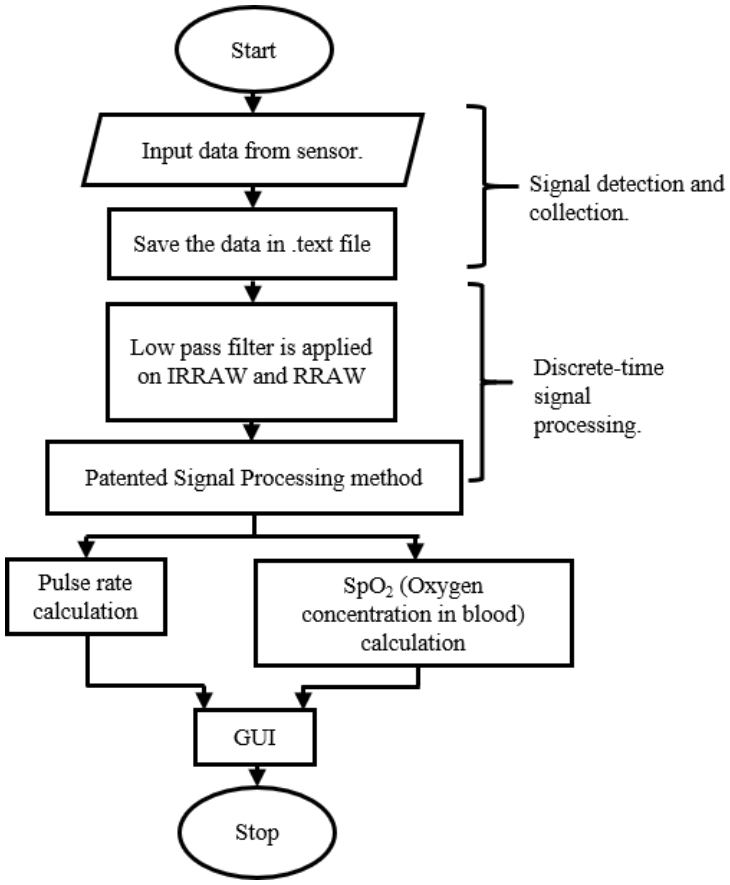

Fig. 4 Signal Processing Algorithm for calculating SpO2, using raw reflected signal from Infrared Laser diode (IRRAW) and Red Laser diode (RRAW).

Ideally, the reflected signal should be as shown in Fig. 5(a), where the peak and valley of the waveform is used for the computation of heart beat and SpO_2 [12]. In actual case when SpO_2 is above 94%, the reflected waveform does resemble the ideal case as shown in Fig 5(b). However, when SpO_2 goes below 94%, as in the case where we intentionally depressed the volunteers' arm 10 minutes at a pressure of 350 mmHg to limit the blood, the expansion and contraction of the blood vessel walls become very small. Since the detection of the SpO_2 is based on the expansion and contraction of the blood vessel walls [12], the signal becomes very weak, and the signal to noise ratio is so small that useful signal cannot be extracted as shown in Fig 5(c). Thus, a special signal processing method has to be developed and the first step in the processing of the saved discrete signals is to filter the noise as shown in Fig 5(d).

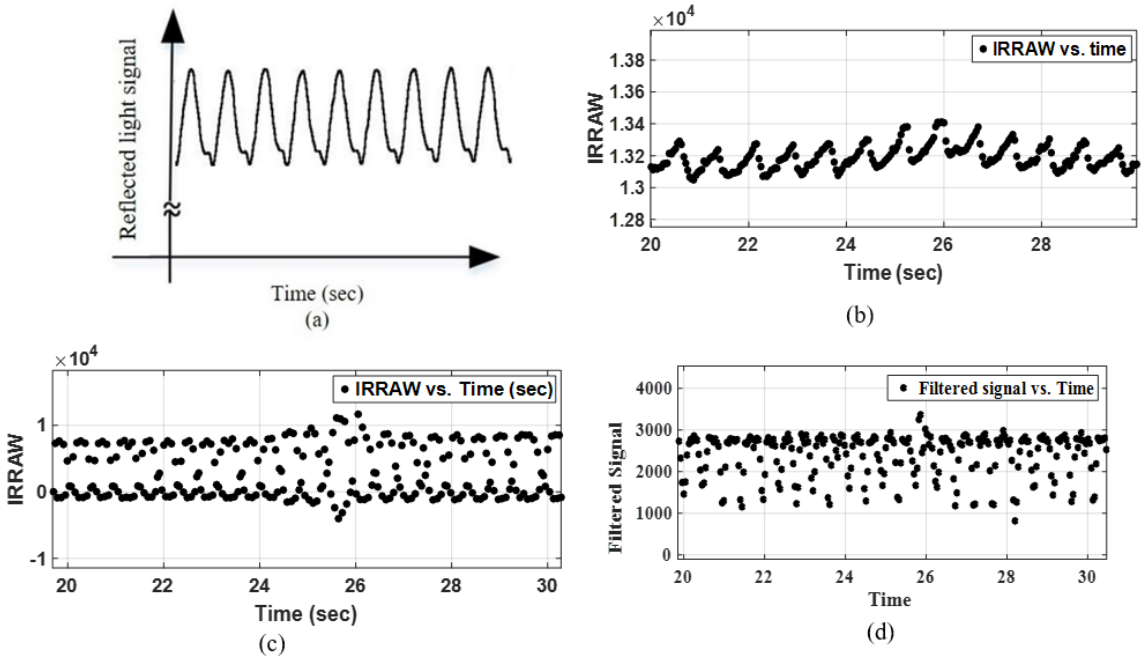

Fig. 5. (a). Ideal reflected from arteries [17], (b). Reflected IRRAW light signals during experiment without depressing the volunteers' arms, (c) Reflected IRRAW light signals during experiment with depressing the volunteers' arms, (d). Filtered signal after applying filter on reflected IRRAW signal.

The setting of the filter is done through Fourier analysis of the signals implemented using the Fast Fourier Transform (FFT) in MATLAB. The noise peaks are found to be prominent after 9 Hz in IRRAW and RRAW signals, as shown in Fig. 6 (a) and (b) respectively.

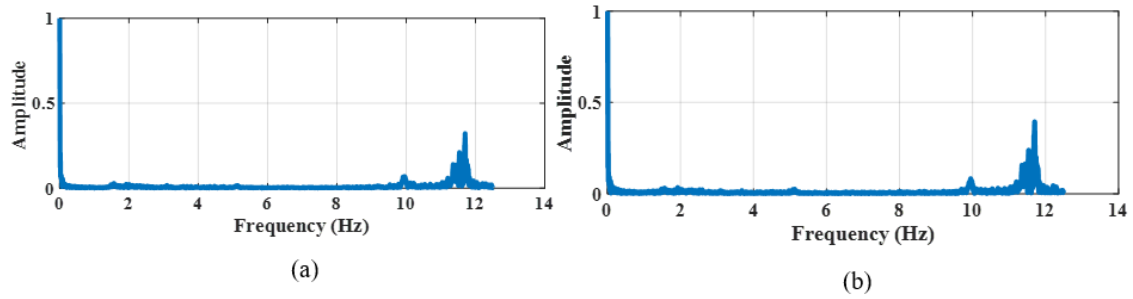

Fig. 6. (a) FFT of the IRRAW signal, (b). FFT of RRAW signal.

To filter out these noise peaks, a low pass filter with the cut off frequency of 9 Hz is applied on the received signals, followed by a mathematical function as shown in Fig.7.

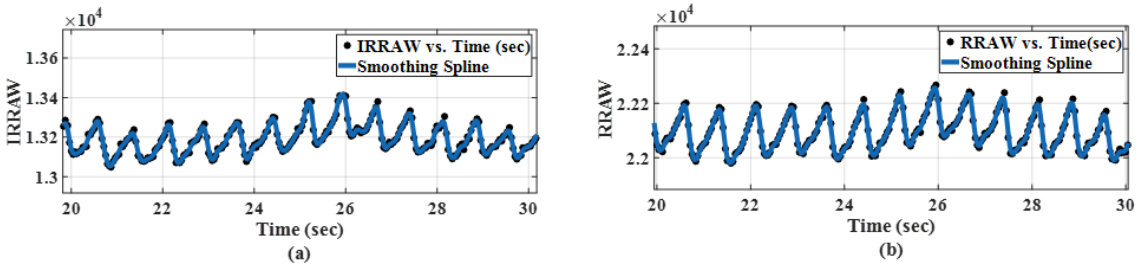

Fig. 7. Mathematical function applied on (a) IRRAW vs time (sec) and (b) RRAW vs time (sec)

Using the filtered and processed IRRAW and RRAW signals, heart rate computation is done by using Eq. (1), where bn is time interval between two peaks as shown in Fig 8(a). As illustrates in Fig. 8, the detection of peaks and valleys are first done using MATLAB, and the time interval between the consecutive peak and valley is calculated.

$$Pulse\ rate\ = \frac{1}{2 \times b_n} \qquad (1)$$

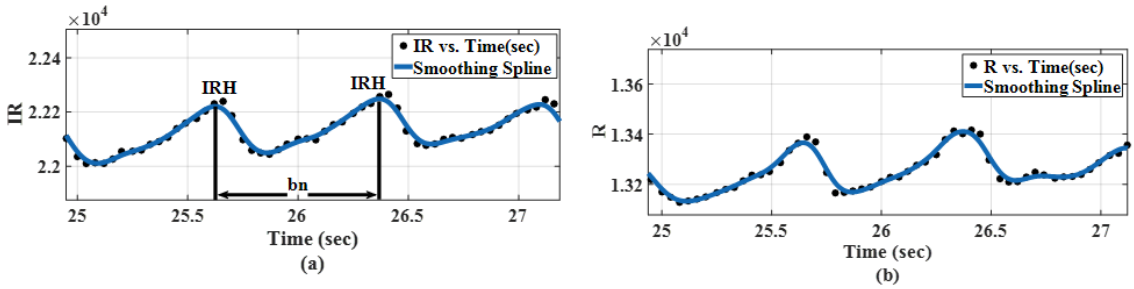

Fig.8. (a) IRH (peak in IRRAW curve for every second) and IRL (valley in IRRAW curve for every second) detection. The time interval between two peaks (IRH) is bn. (b) RH (peak in RRAW curve for every second) and RL (Valley in RRAW curve for every second) detection.

The calculation of the SpO_2 is done using Eq. (3) [18], with the help of Ros (ratio of ratios) [18]. Ros is a variable calculated by taking the natural logarithm of the ratio of the valley (RL) to peak (RH) of the red signal, which is further divided by the natural logarithm of the ratio of the valley (IRL) to peak (IRH) of the infrared signal, as shown in Eq. (2) [19].

$$Ros = \frac{\ln\left(\frac{RL}{RH}\right)}{\ln\left(\frac{IRL}{IRH}\right)} \tag{2}$$

$$SpO_2 = \frac{\varepsilon_{HB}(\lambda_R) - \varepsilon_{HB}(\lambda_{IR})R_{OS}}{\varepsilon_{HB}(\lambda_R) - \varepsilon_{HBO_2}(\lambda_R) + [\varepsilon_{HBO_2}(\lambda_{IR}) - \varepsilon_{HB}(\lambda_{IR})]R_{OS}} \tag{3}$$

In Eq. (2), $\varepsilon_{\mathrm{HB}}(\lambda_R)$ is the extinction coefficient of red light for reduced hemoglobin, $\varepsilon_{\mathrm{HB}}(\lambda_{IR})$is the extinction coefficient of infrared light for reduced hemoglobin, $\varepsilon_{\mathrm{HBO_2}}(\lambda_{IR})$ is the extinction coefficient of infrared light for oxyhemoglobin and $\varepsilon_{\mathrm{HBO_2}}(\lambda_R)$ is the extinction coefficient of red light for oxyhemoglobin. These values are obtained from Fig.9 for the wavelength of the red light (660nm) and infrared (850 nm) LDs used. These wavelengths are measured using Integrated sphere of model LM-ISP 3.4. $\varepsilon_{\mathrm{HBO_2}}(\lambda_R)$, $\varepsilon_{\mathrm{HBO_2}}(\lambda_{IR})$ are obtained from Oxyhemoglobin curve and $\varepsilon_{\mathrm{HB}}(\lambda_R)$, $\varepsilon_{\mathrm{HB}}(\lambda_{IR})$ are obtained from Reduced hemoglobin curve. The narrow chromatic spread of the laser diodes also helps in providing more accurate extinction coefficients for the calculation.

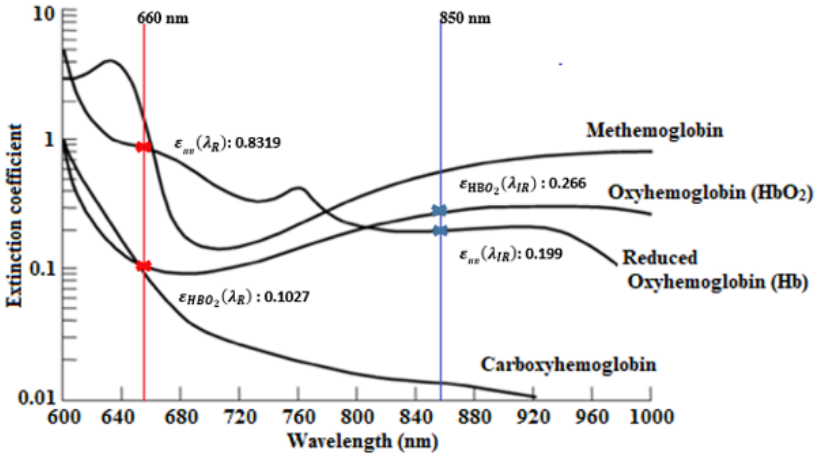

Fig. 9. Extinction coefficients $\varepsilon_{\mathrm{HB}O_2}(\lambda_R)$, $\varepsilon_{\mathrm{HB}O_2}(\lambda_{IR})$, $\varepsilon_{\mathrm{HB}}(\lambda_R)$ and $\varepsilon_{\mathrm{HB}}(\lambda_{IR})$ vs. different light wavelength in human blood [17].

RESULTS AND DISCUSSION

Arterial Blood Gas (ABG) test [21] is used as reference to measure the accuracy of Oximeters. Oximeter developed in this work as well as a commercial oximeter commonly used in hospital are used for testing. In order to detect SpO_2 <94%, the upper arm of the volunteers is pressed for 10 minutes with the pressure of 350 mm Hg, using proximal and distal cuffs to stop the blood flow in the lower arm, as shown in Fig. 10.

Fig.10. Measurement of SpO2, when blood flow is obstructed by the proximal and distal cuffs.

The ABG test is performed by taking blood from the ulnar artery [21], under the supervision of a qualified medical doctor at Chang Gung Memorial Hospital (CGMH), Linkou, Taiwan. The comparison of the test results is shown in Table 2.

TABLE II: Oximeter results and comparison

Person	Condition	SpO_2% (ABG)	SpO_2 % (this work)	Error % (this work)	Measurement Time (this work)	SpO_2 % (commercial Oximeter)	Measurement Time (commercial Oximeter)	Error % (commercial Oximeter)
Volunteer 1	Before upper arm depressed (SpO_2 > 94%)	97	Palm = 97.8	0.8	35 Seconds	Palm = 100	18 seconds	3
			Thumb = 95	2	35 Seconds	Thumb = 99	5 seconds	2
	After Upper arm depressed (SpO_2 < 94%)	66	Palm = 70	4	35 Seconds	Palm = no value	3 minutes	-
			Thumb = 69	3	35 Seconds	Thumb = no value	3 minutes	-
Volunteer 2	Before upper arm depressing (SpO_2 > 94%)	98	Palm = 100	2	35 Seconds	Palm = 100	25 seconds	2
			Thumb = 99	1	35 Seconds	Thumb = 98	15 seconds	1
	After Upper arm depressed (SpO_2 < 94%)	Low	Palm = 78	-	35 Seconds	Palm = no value	3 minutes	-
			Thumb = 81	-	35 Seconds	Thumb = no value	3 minutes	-

ABG test takes around 20 minutes and the process is tedious, Our Oximeter took only 35 seconds with the error rate of ± 2% for SpO_2 > 94% and ± 4% for SpO_2 < 94%. On the other hand, the commercial oximeter can measure SpO_2 > 94% with the error rate of ± 3% within 5-25 seconds but it cannot detect anything for SpO_2 < 94%, even after measuring the SpO_2 for 3 minutes.

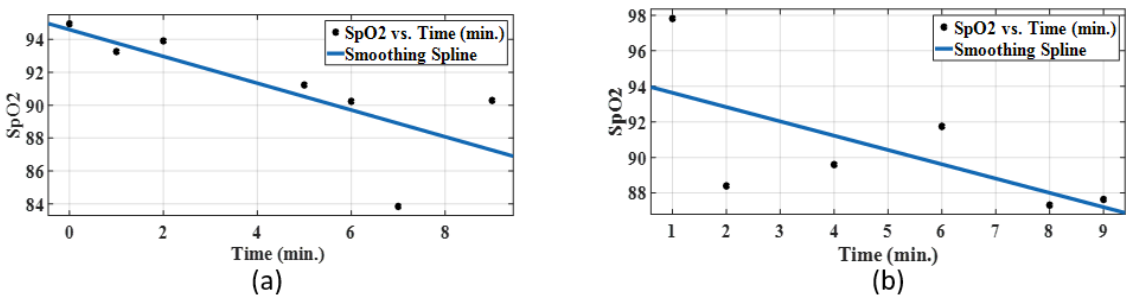

Fig.11 Measurement of SpO_2 for 10 minutes from the palm of (a). volunteer-1 and (b). volunteer-2

The short measurement time to obtain SpO_2 also enable real time monitoring of blood oxygen level. In fact, we do see the time progressing of the SpO_2 decrement when the volunteers' arms were

depressed as shown in Fig. 11. The rate of decrease SpO_2 might be a useful data for physicians in detecting the blood vessel elasticity, and this is beyond the scope of this work.

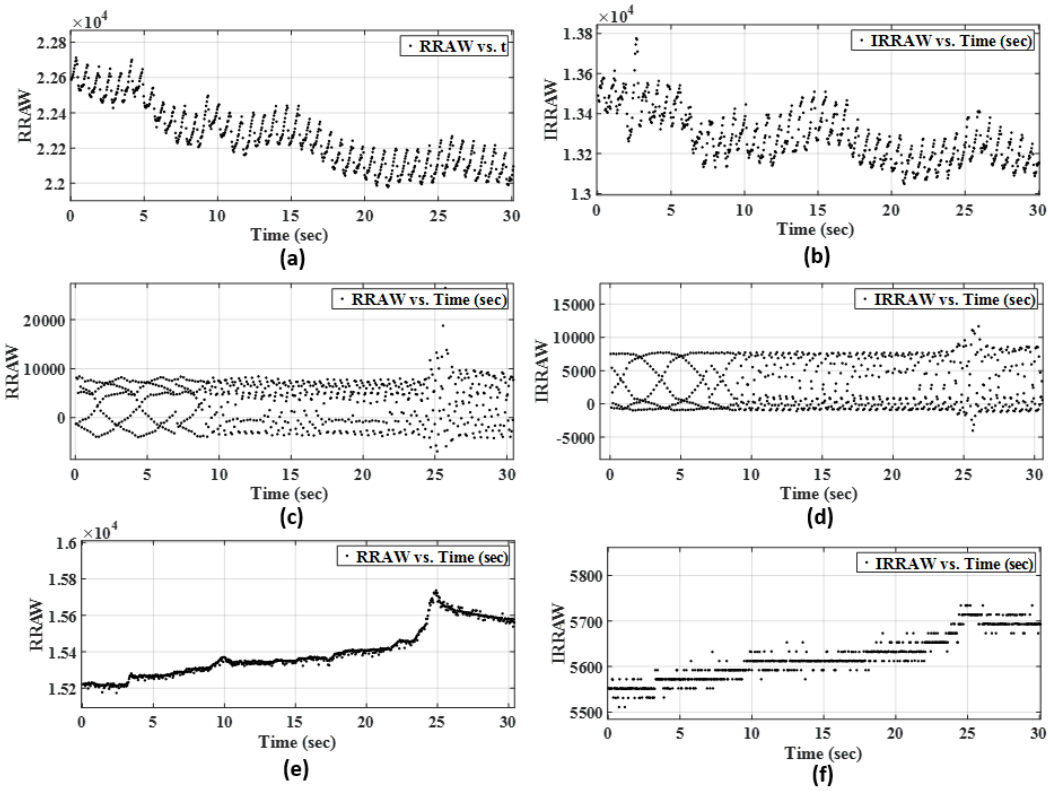

Fig.12 (a) and (b) represent IRRAW and RRAW signals and one can see that they have similar pattern (when blood flow is not obstructed); (c) and (d) represent IRRAW and RRAW signals and again they have similar pattern (when blood flow is obstructed by the proximal and distal cuffs); (e) and (f) IRRAW and RRAW signals have different patterns when there is error during measurement or when there is no object for measurement.

While it is good that the oximeter developed can measure low SpO_2 when the signal level is low, it is equally important to ensure that the signal that we obtain is indeed useful signal instead of noise. In our measurement, we observed that when our oximeter is measuring the correct SpO_2, the IRRAW and RRAW signals have similar patterns as shown in Fig. 12(a) and (b) when upper arms of the volunteers were not depressed and Fig. 12(c) and (d) when upper arms of the volunteers were depressed using proximal and distal cuffs. However, when there is no object or when there is error during measurement as shown by the inconsistent results between the SpO_2 and ABG test, the IRRAW and RRAW signals do not have similar patterns as observed in Fig. 12(e) and (f). With this self-detection capability built in, one can further ensure the accuracy of the SpO_2.

CONCLUSION

In this work, pulse oximeter is designed and developed that is more resilient against light scattering due to the usage of laser diodes, and it can also determine low SpO_2level by using signal processing algorithm. This algorithm also enables oximeter to detect measurement error or error due to null object.

Performance of the developed Oximeter was compared with a commercial oximeter using Arterial Blood Gas test as reference. It is experimentally demonstrated that developed Oximeter can measure the SpO_2 with the range of 60% to 100% with the minimum error of ± 2% for SpO_2 > 94% and ± 4% for SpO_2 < 94%, whilst the commercial oximeter cannot provide any reading when the SpO_2 <94%.

ACKNOWLEDGMENT

We acknowledge the support of the Chang Gung Memorial Hospital, (Taiwan) and Center for Reliability Sciences & Technologies, Chang Gung University (Taiwan). We would like to thank, Vivek Sangwan, Dipesh Kapoor and Udit Narula from Center for Reliability Sciences & Technologies, Chang Gung University (Taiwan) for their technical inputs and insights.

FUNDING

This research was supported in by the Chang Gung Memorial Hospital, Linkou, Taiwan, grant: CMRPG3F0641.

NOMENCLATURE

Ros	Ratio of the ratios
IRH	Peak of the IR signal.
IRL	Valley of the IR signal.
RH	Peak of the Red signal.
RL	Valley of the Red signal.
FFT	Fast Fourier Transform.
bpm	Beats per minute.
IR	Infrared light.

R	Red light.
IRRAW	Raw signal from IR sensor.
RRAW	Raw signal from R sensor.
CGMH	Chang Gung Medical Hospital.
SpO_2	Peripheral capillary oxygen saturation.
$\varepsilon_{\mathrm{HB}O_2}(\lambda_R)$	Extinction coefficient of red light for oxyhemoglobin.
$\varepsilon_{\mathrm{HB}O_2}(\lambda_{IR})$	Extinction coefficient of infrared light for oxyhemoglobin.
$\varepsilon_{\mathrm{HB}}(\lambda_R)$	Extinction coefficient of red light for reduced hemoglobin.
$\varepsilon_{\mathrm{HB}}(\lambda_{IR})$	Extinction coefficient of infrared light for reduced hemoglobin.
bn	Time interval between two peaks.

REFERENCES

[1]. Adler, Jonathan N., Lori A. Hughes, Robert Vtvilecchia, and Carlos A. Camargo Jr. 'Effect of Skin Pigmentation on Pulse Oximetry Accuracy in the Emergency Department'. Academic Emergency Medicine 5, no. 10 (October 1998): 965–70. doi:10.1111/j.1553-2712.1998.tb02772.x.

[2]. Aoyagi, Takuo. 'Pulse Oximetry: Its Invention, Theory, and Future'. Journal of Anesthesia 17, no. 4 (1 November 2003): 259–66. doi:10.1007/s00540-003-0192-6.

[3]. Basaranoglu, Gokcen, Mefkur Bakan, Tarik Umutoglu, Seniyye Ulgen Zengin, Kadir Idin, and Ziya Salihoglu. 'Comparison of SpO_2 Values from Different Fingers of the Hands.' SpringerPlus 4 (2015): 561. doi:10.1186/s40064-015-1360-5.

[4]. Baura, Gail D. Medical Device Technologies : A Systems Based Overview Using Engineering Standards. Academic, 2011.

[5]. Birnbaum, Sam. 'Pulse Oximetry: Identifying Its Applications, Coding, and Reimbursement'. Chest 135, no. 3 (1 March 2009): 838–41. doi:10.1378/CHEST.07-3127.

[6]. Chen, Hsiao-Wen, Li-Chueh Weng, Ta-Min Wang, and Kwai-Fong Ng. 'Potential Use of Pulse Oximetry for the Diagnosis of Testicular Torsion'. JAMA Pediatrics 168, no. 6 (1 June 2014): 578. doi:10.1001/jamapediatrics.2014.86.

[7]. Gonzalez, Anthony L., and Lori S. Waddell. 'Blood Gas Analyzers'. Topics in Companion Animal Medicine 31, no. 1 (1 March 2016): 27–34. doi:10.1053/J.TCAM.2016.05.001.

[8]. Humphreys, Kenneth, Tomas Ward, and Charles Markham. 'Noncontact Simultaneous Dual Wavelength Photoplethysmography: A Further Step toward Noncontact Pulse Oximetry'. Review of Scientific Instruments 78, no. 4 (April 2007): 044304. doi:10.1063/1.2724789.

[9]. Isaacson, Philip O., David W. Gadtke, Vernon D. Heidner, and Neal F. Nordling. Pulse oximeter with circuit leakage and ambient light compensation, issued 23 July 1991. http://www.freepatentsonline.com/RE33643.html.

[10]. Jubran, Amal. 'Pulse Oximetry.' Critical Care (London, England) 19, no. 1 (16 July 2015): 272. doi:10.1186/s13054-015-0984-8.

[11]. Kyriacou, Panayiotis A. 'Pulse Oximetry in the Oesophagus.' Undefined, 2006. https://www.semanticscholar.org/paper/Pulse-oximetry-in-the-oesophagus.-Kyriacou/f62a7f308bb6ad28921394fbe7fa51650b4e4fbe.

[12]. Nitzan, Meir, Salman Noach, Elias Tobal, Yair Adar, Yaacov Miller, Eran Shalom, and Shlomo Engelberg. 'Calibration-Free Pulse Oximetry Based on Two Wavelengths in the Infrared - a Preliminary Study.' Sensors (Basel, Switzerland) 14, no. 4 (23 April 2014): 7420–34. doi:10.3390/s140407420.

[13]. Paleček, Emil, and Vlastimil Dorčák. 'Label-Free Electrochemical Analysis of Biomacromolecules'. Applied Materials Today 9 (1 December 2017): 434–50. doi:10.1016/J.APMT.2017.08.011.

[14]. Rajadhyaksha, Milind, R. Rox Anderson, and Robert H. Webb. 'Video-Rate Confocal Scanning Laser Microscope for Imaging Human Tissues in Vivo'. Applied Optics 38, no. 10 (1 April 1999): 2105. doi:10.1364/AO.38.002105.

[15]. Salem, Kyle A. 'Motion Correction for MR Imaging'. Accessed 23 July 2018. http://mriquestions.com/uploads/3/4/5/7/34572113/motion_hot_topics_broc-00017164.pdf.

[16]. Severinghaus, John W., and Poul B. Astrup. 'History of Blood Gas Analysis. VI. Oximetry'. Journal of Clinical Monitoring 2, no. 4 (October 1986): 270–88. doi:10.1007/BF02851177.

[17]. Severinghaus, John W., and Yoshiyuki Honda. 'History of Blood Gas Analysis. VII. Pulse Oximetry'. Journal of Clinical Monitoring 3, no. 2 (April 1987): 135–38. doi:10.1007/BF00858362.

[18]. Shokouhian, Mohsen, Richard Morling, and Izzet Kale. 'Interference Resilient Sigma Delta-Based Pulse Oximeter'. IEEE Transactions on Biomedical Circuits and Systems 10, no. 3 (June 2016): 623–31. doi:10.1109/TBCAS.2015.2501359.

[19]. Weindler, J., M. Winter, and C. Zapf. 'The Relationship of SpO_2 93%–95% to Arterial Blood Gases and Pulmonary Function Parameters'. In New Aspects on Respiratory Failure, 329–34. Berlin, Heidelberg: Springer Berlin Heidelberg, 1992. doi:10.1007/978-3-642-74943-8_34.

[20]. Yan, Yong-sheng, Carmen CY Poon, and Yuan-ting Zhang. 'Reduction of Motion Artifact in Pulse Oximetry by Smoothed Pseudo Wigner-Ville Distribution'. Journal of NeuroEngineering and Rehabilitation 2, no. 1 (1 March 2005): 3. doi:10.1186/1743-0003-2-3.

[21]. Yu, Jiashun, Stuart A. Henrys, Colin Brown, Ivor Marsh, Garret Duffy, J. Yu, S.A. Henrys, C. Brown, I. Marsh, and G. Duffy. 'A Combined Boundary Integral and Lambert's Law Method for Modelling Multibeam Backscatter Data from the Seafloor'. Continental Shelf Research 103, no. 103 (July 2015): 60–69. doi:10.1016/j.csr.2015.04.020.

Figure Captions List

Fig 1	Research methodology flow chart.
Fig 2	Hardware architecture of oximeter.
Fig 3	(a). Oximeter sensor's probe head, (b). Arduino driven circuit for SpO_2 measurement
Fig 4	Signal Processing Algorithm for calculating SpO_2, using raw reflected signal from Infrared Laser diode (IRRAW) and Red Laser diode (RRAW).
Fig 5	(a). Ideal reflected from arteries [17], (b). Reflected IRRAW light signals during experiment without depressing the volunteers' arms, (c) Reflected IRRAW light signals during experiment with depressing the volunteers' arms, (d). Filtered signal after applying filter on reflected IRRAW signal.
Fig 6	(a) FFT of the IRRAW signal, (b). FFT of RRAW signal.
Fig 7	Mathematical function applied on (a) IRRAW vs time (sec) and (b) RRAW vs time (sec)
Fig 8	(a) IRH (peak in IRRAW curve for every second) and IRL (valley in IRRAW curve for every second) detection. The time interval between two peaks (IRH) is bn. (b) RH (peak in RRAW curve for every second) and RL (Valley in RRAW curve for every second) detection.
Fig 9	Extinction coefficients $\varepsilon_{\mathrm{HBO}_2}(\lambda_R)$, $\varepsilon_{\mathrm{HBO}_2}(\lambda_{IR})$, $\varepsilon_{\mathrm{HB}}(\lambda_R)$ and $\varepsilon_{\mathrm{HB}}(\lambda_{IR})$ vs. different light wavelength in human blood [17]
Fig 10	Measurement of SpO_2, when blood flow is obstructed by the proximal and distal cuffs.
Fig 11	Measurement of SpO_2 for 10 minutes from the palm of (a). volunteer-1 and (b). volunteer-2
Fig 12	(a) and (b) represent IRRAW and RRAW signals and one can see that they have similar pattern (when blood flow is not obstructed); (c) and (d) represent IRRAW and RRAW signals and again they have similar pattern (when blood flow is obstructed by the proximal and distal cuffs); (e) and (f) IRRAW and RRAW signals have different patterns when there is error during measurement or when there is no object for measurement.

Table Caption List

Table 1	Limitations and their reported solutions for the commercial oximeter
Table 2	Oximeter results and comparison